Inorganic Chemistry
Article

Inorg. Chem. **2010**, *49*, 295–301 **295**
DOI: 10.1021/ic902039g

Computationally Designed Metal-Free Hydrogen Activation Site: Reaching the Reactivity of Metal−Ligand Bifunctional Hydrogenation Catalysts

Gang Lu, Haixia Li, Lili Zhao, Fang Huang, and Zhi-Xiang Wang*

College of Chemistry and Chemical Engineering, Graduate University of Chinese Academy of Sciences, Beijing, 100049, China

Received October 14, 2009

In this study, a strategy to design a metal-free hydrogen activation site has been proposed. On the basis of our so-called sp^3 carbon bridged FLPs (Frustrated Lewis Pairs), we first hypothesized that a more reactive activation site should arrange the nitrogen lone pair and the boron vacant orbital to lie in the same plane face-to-face, because such orbital orientations can simultaneously enhance the interaction between the nitrogen lone pair and the H_2 σ^* antibonding orbital and the interaction between the boron vacant orbital and the H_2 σ bonding electrons. To verify that such an active site is achievable, we then computationally designed molecules and studied their reactions with hydrogen. The energetic results show the designed molecules are indeed more reactive than the sp^3 carbon bridged FLPs. Some of the hydrogen activations reach kinetics and thermodynamics comparable with those of the hydrogen activations mediated by the well-known metal−ligand bifunctional hydrogenation catalysts. The designed molecules could be the targets for experimental synthesis. The pattern of the proposed active site can be based to design similar molecules for metal-free hydrogenations.

Introduction

Hydrogen activation is the preliminary step for using H_2 as chemical feedstock.[1] While the step can be easily completed by using transition metal (TM) complexes,[1,2] chemists are interested in developing a TM-free way to activate H_2 because of the economic and environmental concerns.[3] The chemistry of FLPs (Frustrated Lewis pairs) recently discovered by Stephan and co-workers[4] has further inspired both experimental[5−9] and computational[10] chemists in this field. On the basis of the FLP prototype, $P(t\text{Bu})_3/B(C_6F_5)_3$ (**1** in Scheme 1),[5a] more and more FLPs were prepared.[5−8] FLPs have unusual reactivity to activate H_2[5−8] and other small molecules.[9] The facile hydrogen activation character of FLPs has been used to realize metal-free direct catalytic hydrogenations,[8] the important chemical processes often catalyzed by TM complexes such as metal−ligand bifunctional hydrogenation catalysts (MLBHCs, e.g., **2**).[11] Recently, Pápai's group[10b] elucidated the catalytic mechanism of the imine (tBuN=CHPh) hydrogenation mediated by $B(C_6F_5)_3$, and Privalov[10f] presented his rationalization on

*To whom correspondence should be addressed. E-mail: zxwang@gucas.ac.cn.

(1) Tolman, W. B. *Activation of Small Molecules*; Wiley-VCH: Weinheim, 2006.

(2) (a) Kubas, G. J. *Chem. Rev.* **2007**, *107*, 4152. (b) Kubas, G. J. *Metal Dihydrogen and σ-Bond Complexes*; Kluwer Academic/Plenum Publishers: NewYork, 2001. (c) Crabtree, R. H. *The organometallic Chemistry of the Transition Metals*, 4th ed.; Wiley-Interscience: New Jersey, 2005.

(3) (a) Xiao, Z. L.; Hauge, R. H.; Margrave, J. L. *Inorg. Chem.* **1993**, *32*, 642. (b) Himmel, H. J. *J. Chem. Soc., Dalton Trans.* **2002**, 2678. (c) Himmel, H.; Vollet, J. *Organometallics* **2002**, *21*, 5972. (d) Himmel, H. J. *Dalton Trans.* **2003**, 3639. (e) Chan, B.; Radom, L. *J. Am. Chem. Soc.* **2005**, *127*, 2443. (f) Spikes, G. H.; Fettinger, J. C.; Power, P. P. *J. Am. Chem. Soc.* **2005**, *127*, 12232. (g) Chan, B.; Radom, L. *J. Am. Chem. Soc.* **2006**, *128*, 5322. (h) Zhong, G.; Chan, B.; Radom, L. *J. Am. Chem. Soc.* **2007**, *129*, 924. (i) Chan, B.; Radom, L. *J. Am. Chem. Soc.* **2008**, *130*, 9790. (j) Peng, Y.; Brynda, M.; Ellis, B. D.; Fettinger, J. C.; Rivard, E.; Power, P. P. *Chem. Commun.* **2008**, 6042. (k) Peng, Y.; Ellis, B. D.; Wang, X. P.; Power, P. P. *J. Am. Chem. Soc.* **2008**, *130*, 12268. (l) Kenward, A. L.; Piers, W. E. *Angew. Chem., Int. Ed.* **2008**, *47*, 38. (m) Zhu, Z. L.; Wang, X. P.; Peng, Y.; Lei, H.; Fettinger, J. C.; Rivard, E.; Power, P. P. *Angew. Chem., Int. Ed.* **2009**, *48*, 2031. (n) Zhong, G.; Chan, B.; Radom, L. *Org. Lett.* **2009**, *11*, 749. (o) Bettinger, H. F.; Filthaus, M.; Neuhaus, P. *Chem. Commun.* **2009**, 2186. (p) Ito, S.; Miura, J.; Morita, N.; Yoshifuji, M.; Arduengo, A. J. *Inorg. Chem.* **2009**, *48*, 8063. (q) Wang, Y.; Ma, J. *J. Organomet. Chem.* **2009**, *694*, 2567. (r) Moc, J. *Eur. Phys. J. D* **2009**, *53*, 309.

(4) (a) Welch, G. C.; Juan, R. R. S.; Masuda, J. D.; Stephan, D. W. *Science* **2006**, *314*, 1124. (b) Stephan, D. W. *Org. Biomol. Chem.* **2008**, *6*, 1535.

(5) B/P FLPs: (a) Welch, G. C.; Stephan, D. W. *J. Am. Chem. Soc.* **2007**, *129*, 1880. (b) Ullrich, M.; Lough, A. J.; Stephan, D. W. *J. Am. Chem. Soc.* **2009**, *131*, 52. (c) Ramos, A.; Lough, A. J.; Stephan, D. W. *Chem. Commun.* **2009**, 1118. (d) Spies, P.; Kehr, G.; Bergander, K.; Wibbeling, B.; Fröhlich, R.; Erker, G. *Dalton Trans.* **2009**, 1534. (e) Spies, P.; Erker, G.; Kehr, G.; Bergander, K.; Fröehlich, R.; Grimme, S.; Stephan, D. W. *Chem. Commun.* **2007**, 5072. (f) Welch, G. C.; Cabrera, L.; Chase, P. A.; Hollink, E.; Masuda, J. D.; Wei, P. R.; Stephan, D. W. *Dalton Trans.* **2007**, 3407. (g) Mömming, C. M.; Frömel, S.; Kehr, G.; Fröhlich, R.; Grimme, S.; Erker, G. *J. Am. Chem. Soc.* **2009**, *131*, 12280. (h) Jiang, C.; Blacque, O.; Berke, H. *Organometallics* **2009**, *28*, 5233.

(6) B/Carbene FLPs: (a) Holschumacher, D.; Bannenberg, T.; Hrib, C. G.; Jones, P. G.; Tamm, M. *Angew. Chem., Int. Ed.* **2008**, *47*, 7428. (b) Chase, P. A.; Stephan, D. W. *Angew. Chem., Int. Ed.* **2008**, *47*, 7433. (c) Chase, P. A.; Gille, A. L.; Gilbert, T. M.; Stephan, D. W. *Dalton Trans.* **2009**, 7179. (d) Holschumacher, D.; Taouss, C.; Bannenberg, T.; Hrib, C. G.; Daniliuc, C. G.; Jones, P. G.; Tamm, M. *Dalton Trans.* **2009**, 6927.

Published on Web 12/03/2009

Scheme 1. Schematic Representations of **1**−**5** and **9**

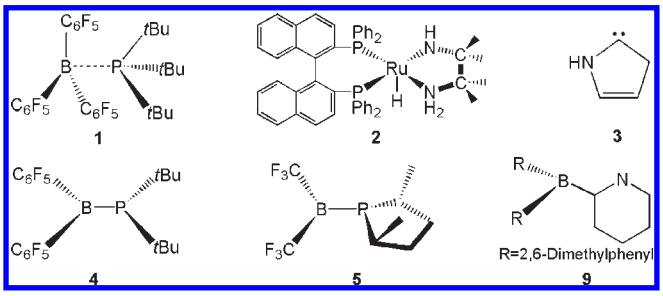

the catalytic hydrogenation of imine (tBuN=CHPh) by phosphonium borate zwitterion.

Bertrand's group[12] uncovered that the stable mono(amino)carbenes (exemplified by the model **3**) alone can also activate H_2 and NH_3 under ambient conditions. While FLPs have differentiable acidic and basic centers, the carbene carbon center functions as both electron donor and electron acceptor, which is similar to the TM-mediated hydrogen activations.[1,2]

The phosphinoborane (e.g., $(t\text{Bu})_2\text{PB}(\text{C}_6\text{F}_5)_2$, (**4**))[13] represents another approach of metal-free hydrogen activation. In **4**, the acidic B-center and the basic P-center are bound together via a covalent bond, rather than the nonbonding interactions in **1**. This is similar to MLBHCs.[11] As exemplified by **2**, the acidic Ru-center and the basic N-center of the ligand are bound together. Computational studies[13] rationalized that the facile hydrogen activation of **4** is due to the highly polarized P−B π bond caused by the mismatch of orbital energies of the lone pair of the P-center and the vacant orbital of the B-center. Privalov[10g] computationally explored the possibility of using **4** to reduce alcohol to ketone. Using **4** as a prototype, he and co-workers[10h] optimized the substituents to enhance hydrogen activation reactivity and proposed a more reactive analogue (**5**).

The often-used Lewis acid, $B(C_6F_5)_3$, is able to pair with both phosphorus- and nitrogen-centered Lewis bases to form effective FLPs. We recently found that the hydrogen activation principle based on **4** can not be extended to molecules with B−N π bond capable of activating H_2.[14] Our calculations[14] showed a high activation barrier ($\Delta E^{\ddagger}$ = 42.7 kcal/mol at the M05-2X/6-311++G**+ZPE level) for the model reaction BH_2NH_2 (**6**) + $H_2 \rightarrow BH_3NH_3$. This barrier is much higher than the 18.5 kcal/mol of BH_2PH_2 (**7**, the model of **4**). This computational prediction awaits experimental verifications. To improve the reactivity of **6**, we proposed to insert a CH_2 bridge into the B−N bond of **6**, giving a new form of FLP **8** ($BH_2CH_2NH_2$, a model for the generic sp^3 carbon bridged FLPs). The effectiveness of the CH_2 bridge is indicated by the much lower barrier of **8** (12.0 kcal/mol) than the 42.7 kcal/mol of **6**. Although the effectiveness of the CH_2 bridge is evident, it is desirable to further improve its reactivity because the hydrogen activation is often the rate-determining step for direct catalytic hydrogenations. Moreover, although the model **8** has a low barrier (12.0 kcal/mol), it is a computational model. Proper substituents are required to avoid forming Lewis acid−base complexes (see below). The substitutions often increase the activation barriers. For example, our previously reported **9** has an energy barrier (17.4 kcal/mol) higher than the 12.0 kcal/mol of the model **8**.[14] In this study, based on **8**, we optimized the hydrogen activation site of **8** to enhance its reactivity. As shown below, the designed molecules containing such a new active site have the reactivity comparable with that of the well-known MLBHC (**2**).

Computational Details

The M05−2X[15] functional was used for all density functional theory (DFT) calculations. The structures of the reactants (i.e., the designed molecules), the transitions states, and the products involved in the hydrogen activations were optimized and subsequently characterized by frequency analysis calculations at the M05−2X/6-31G** level. The reactants and products were confirmed to be minima, and the transition states to be the first-order saddle points. The structures were then refined by the M05−2X/6-311++G** optimizations. The solvent effects of toluene (the often used solvent in the experimental study) were accounted by the IEFPCM (integral equation formalism polarizable continuum solvent model)[16] model with the UFF atomic radii.

(7) For B/N FLP H_2 activation: (a) Sumerin, V.; Schulz, F.; Nieger, M.; Leskelä, M.; Repo, T.; Rieger, B. *Angew. Chem., Int. Ed.* **2008**, *47*, 6001. (b) Geier, S. J.; Stephan, D. W. *J. Am. Chem. Soc.* **2009**, *131*, 3476. (c) Geier, S. J.; Gille, A. L.; Gilbert, T. M.; Stephan, D. W. *Inorg. Chem.* **2009**, *48*, 10466.

(8) For direct catalytic hydrogenations: (a) Wang, H. D.; Fröhlich, R.; Kehr, G.; Erker, G. *Chem. Commun.* **2008**, 5966. (b) Sumerin, V.; Schulz, F.; Atsumi, M.; Wang, C.; Nieger, M.; Leskelä, M.; Repo, T.; Pyykkö, P.; Rieger, B. *J. Am. Chem. Soc.* **2008**, *130*, 14117. (c) Spies, P.; Schwendemann, S.; Lange, S.; Kehr, G.; Fröhlich, R.; Erker, G. *Angew. Chem., Int. Ed.* **2008**, *47*, 7543. (d) Axenov, K. V.; Kehr, G.; Fröhlich, R.; Erker, G. *J. Am. Chem. Soc.* **2009**, *131*, 3454. (e) Axenov, K. V.; Kehr, G.; Fröhlich, R.; Erker, G. *Organometallics* **2009**, *28*, 5148. (f) Chase, P. A.; Welch, G. C.; Jurca, T.; Stephan, D. W. *Angew. Chem., Int. Ed.* **2007**, *46*, 8050. (g) Chase, P. A.; Jurca, T.; Stephan, D. W. *Chem. Commun.* **2008**, 1701. (h) Sumerin, V.; Schulz, F.; Nieger, M.; Atsumi, M.; Wang, C.; Leskelä, M.; Pyykkö, P.; Repo, T.; Rieger, B. *J. Organomet. Chem.* **2009**, *694*, 2654. (i) Chen, D. J.; Klankermayer, J. *Chem. Commun.* **2008**, 2130. (j) Jiang, C.; Blacque, O.; Berke, H. *Chem. Commun.* **2009**, 5518.

(9) Other small molecules activations: (a) Stephan, D. W. *Dalton Trans.* **2009**, 3129, and references cited therein. (b) Mömming, C. M.; Otten, E.; Kehr, G.; Fröhlich, R.; Grimme, S.; Stephan, D. W.; Erker, G. *Angew. Chem., Int. Ed.* **2009**, *48*, 6643. (c) Welch, G. C.; Prieto, R.; Dureen, M. A.; Lough, A. J.; Labeodan, O. A.; Höltrichter-Rössmann, T.; Stephan, D. W. *Dalton Trans.* **2009**, 1559. (d) Ullrich, M.; Seto, K. S. H.; Lough, A. J.; Stephan, D. W. *Chem. Commun.* **2009**, 2335. (e) Otten, E.; Neu, R. C.; Stephan, D. W. *J. Am. Chem. Soc.* **2009**, *131*, 9918. (f) Dureen, M. A.; Stephan, D. W. *J. Am. Chem. Soc.* **2009**, *131*, 8396.

(10) (a) Rokob, T. A.; Hamza, A.; Stirling, A.; Soós, T.; Pápai, I. *Angew. Chem., Int. Ed.* **2008**, *47*, 2435. (b) Rokob, T. A.; Hamza, A.; Stirling, A.; Pápai, I. *J. Am. Chem. Soc.* **2009**, *131*, 2029. (c) Hamza, A.; Stirling, A.; Rokob, T. A.; Pápai, I. *Int. J. Quantum Chem.* **2009**, *109*, 2416. (d) Rokob, T. A.; Hamza, A.; Papai, I. *J. Am. Chem. Soc.* **2009**, *131*, 10701. (e) Stirling, A.; Hamza, A.; Rokob, T. A.; Pápai, I. *Chem. Commun.* **2008**, 3148. (f) Privalov, T. *Dalton Trans.* **2009**, 1321. (g) Privalov, T. *Chem.—Eur. J.* **2009**, *15*, 1825. (h) Nyhlén, J.; Privalov, T. *Eur. J. Inorg. Chem.* **2009**, 2759. (i) Privalov, T. *Eur. J. Inorg. Chem.* **2009**, 2229. (j) Nyhlén, J.; Privalov, T. *Dalton Trans.* **2009**, 5780. (k) Guo, Y.; Li, S. *Inorg. Chem.* **2008**, *47*, 6212. (l) Guo, Y.; Li, S. *Eur. J. Inorg. Chem.* **2008**, 2501.

(11) For examples: (a) Noyori, R.; Ohkuma, T. *Angew. Chem., Int. Ed.* **2001**, *40*, 40. (b) Noyori, R. *Angew. Chem., Int. Ed.* **2002**, *41*, 2008. (c) Ikariya, T.; Murata, K.; Noyori, R. *Org. Biomol. Chem.* **2006**, *4*, 393. (d) Abdur-Rashid, K.; Clapham, S. E.; Hadzovic, A.; Harvey, J. N.; Lough, A. J.; Morris, R. H. *J. Am. Chem. Soc.* **2002**, *124*, 15104. (e) Clapham, S. E.; Hadzovic, A.; Morris, R. H. *Coord. Chem. Rev.* **2004**, *248*, 2201. (f) De Iuliis, M. Z.; Morris, R. H. *J. Am. Chem. Soc.* **2009**, *131*, 11263.

(12) Frey, G. D.; Lavallo, V.; Donnadieu, B.; Schoeller, W. W.; Bertrand, G. *Science* **2007**, *316*, 439.

(13) Geier, S. J.; Gilbert, T. M.; Stephan, D. W. *J. Am. Chem. Soc.* **2008**, *130*, 12632.

(14) Wang, Z.-X.; Lu, G.; Li, H. X.; Zhao, L. *Chin. Sci. Bull.* **2009**, in press.

(15) (a) Zhao, Y.; Schultz, N. E.; Truhlar, D. G. *J. Chem. Theory Comput.* **2006**, *2*, 364. (b) Zhao, Y.; Truhlar, D. G. *Acc. Chem. Res.* **2008**, *41*, 157.

(16) Tomasi, J.; Mennucci, B.; Cances, E. *J. Mol. Struct.-THEOCHEM* **1999**, *464*, 211.

Scheme 2. Illustration of Constructing the Hydrogen Activation Site

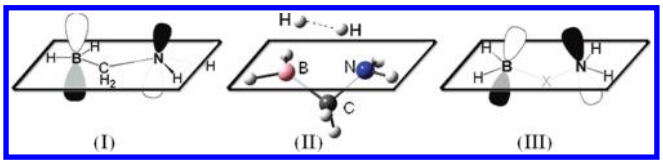

The IEFPCM calculations were carried out at the M05−2X/6-311++G** level at the gas phase M05−2X/6-311++G** geometries. The M05−2X/6-31G** harmonic frequencies were used for thermal and entropic corrections at 297.15 K and 1 atm. The possible dimers or adducts were optimized and characterized at the M05−2X/6-31G** level. When necessary, the BSSE (basis set superposition errors)[17] corrections, calculated by the standard BSSE procedure, were also considered. All the calculations were performed by using Gaussian 03.[18]

Results and Discussion

The FLPs, stable mono(amino)carbenes, phosphinoboranes, and TM complexes (including MLBHCs) all share the underlying principle of using acid/base bifunctional reactivity to activate hydrogen. Our sp^3 carbon-bridged FLPs[14] are not exceptions to this basic principle. On the basis of the model **8** ($BH_2CH_2NH_2$), we reasoned two approaches to improve its reactivity. First, our study[14] showed that the sp^3 carbon bridged B/N FLP cannot be extended to sp^3 carbon bridged B/P FLP, implying there must be an optimal match among the acidic center, basic center, and bridge. We thus can improve the reactivity by matching the three components optimally. It is interesting to note the opposite extendability of sp^3 carbon bridged B/N FLPs and the polarized B−P π bond-based FLPs. Second, one can tune the orbital orientations of the nitrogen lone pair and the boron vacant orbital. Thus, the nitrogen lone pair and boron vacant orbital can interact with the σ^* antibonding orbital and the σ bonding electrons of H_2 more effectively, respectively. The second approach motivated the present study.

The implementation of the second approach is based on the orientations of the frontier molecular orbitals, shown by **I** (i.e., **8**) in Scheme 2, and the structure (**II**) of the hydrogen activation transition state. In **I** the boron vacant orbital is nearly perpendicular to the BCN plane and the nitrogen lone pair is tilted to the plane. Such orientations are not optimal for simultaneously and most efficiently utilizing the acid/base bifunctional reactivity. In the transition state (**II**), the dihydrogen tends to be coplanar with the B···N axis.[14] Therefore, we hypothesized that **III** is a better hydrogen activation site in which the nitrogen lone pair and the boron vacant orbital are oriented in the same plane face-to-face.

III is just an imaginary hydrogen activation site. Can such an active site be achievable? We found that simply replacing the CH_2 linkage in **I** with other groups could not result in the desired arrangement. Proper constructions of chemical scaffolds are needed. After repeatedly guessing and checking, the molecules (**10M**−**13M** in Figure 1) were found capable of maintaining the desired active sites. They are all minima with C_s symmetry and the orbital orientations described by **III** (see Supporting Information, SI1). In **10M** and **11M**, the planar trigonal arrangements of sp^2 carbons help to maintain the orbital orientations. Although the bridging nitrogen atoms in **12M** and **13M** are not sp^2 hybridized, the planarity of the nitrogen atoms because of aromaticity also make them function like sp^2 carbons. **13M** indicates that the strategy can also be applied to construct bridged B/C:(carbene carbon center) FLP. Interestingly, as illustrated in Figure 1, **10M**−**13M** are all composed of the experimentally accessible chemical frameworks (3-Borabicyclo[3.3.1]nonane (3-BBN), 3-Azabicyclo[3.3.1]nonane (3-ABN), ethylene, pyridine, pyrazole, and di(amino)carbene). This feature could be an implication for their experimental realizations.

10M−**13M** possess the desired active sites, but they are not experimentally operable because the active sites can be deactivated because of dimerization. Stephan's group has demonstrated that the analogues of **4**, $R_2PB(C_6F_5)_2$ (R = Et, Ph), could not activate H_2 because of the formation of dimers.[13] The dimerization issue can be overcome by adding proper substituents. As shown by **10**−**12**(Figure 1), the methyl groups on 3-BBN and 3-ABN domains and *t*Bu on pyridine and pyrazole domains are sterically demanding enough to prevent the formation of dimers. **12a**, which has the same substituents on 3-BBN domain as those of **10** and **11**, can form dimers. After examining **13a**−**13d**, we used a five-membered ring and two *t*Bu groups on 3-BBN domains to overcome dimerization, which resulted in **13**.

The energetic and geometric results to verify that **10**−**13** can not be dimerized are detailed in the Supporting Information, SI2. We briefly mention the following two aspects. (i) Two types of dimers were considered. One type contains two B−N (**10**−**12**) or B−C (**13**) dative bonds and the other only has one B−N or B−C dative bond. (ii) To locate the possible dimers, the initial input structures for DFT optimizations were first obtained by partial AM1 optimizations with the assumed dative bonds fixed to be about 1.60 Å. The procedure can avoid missing possible dimers because of improper initial structure input. To examine this, we applied the procedure to the experimental compound **4**. No stable dimer was found though a strained dimer can be obtained. The strained dimer is 25.7 kcal/mol less stable than the two separated monomers. However, the application of the procedure to **5** led to a dimer with two B−P dative bonds, which is 62.2 kcal/mol (after ZPE and BSSE corrections) more stable than two separate monomers. Therefore, further modifications are necessary for an experimental operation to demonstrate that **5** is more reactive than **4**.

To investigate the reactivity of **10**−**13** in activating H_2, the reactions of **10**−**13** with H_2 have been studied. The optimized structures of **10**−**13**, the transition states (**10TS**−**13TS**), and

(17) (a) Boys, S. F.; Bernardi, F. *Mol. Phys.* **1970**, *19*, 553. (b) Simon, S.; Duran, M.; Dannenberg, J. J. *J. Chem. Phys.* **1996**, *105*, 11024.

(18) Frisch, M. J.; Trucks, G. W.; Schlegel, H. B.; Scuseria, G. E.; Robb, M. A.; Cheeseman, J. R.; Montgomery, Jr., J. A.; Vreven, T.; Kudin, K. N.; Burant, J. C.; Millam, J. M.; Iyengar, S. S.; Tomasi, J.; Barone, V.; Mennucci, B.; Cossi, M.; Scalmani, G.; Rega, N.; Petersson, G. A.; Nakatsuji, H.; Hada, M.; Ehara, M.; Toyota, K.; Fukuda, R.; Hasegawa, J.; Ishida, M.; Nakajima, T.; Honda, Y.; Kitao, O.; Nakai, H.; Klene, M.; Li, X.; Knox, J. E.; Hratchian, H. P.; Cross, J. B.; Bakken, V.; Adamo, C.; Jaramillo, J.; Gomperts, R.; Stratmann, R. E.; Yazyev, O.; Austin, A. J.; Cammi, R.; Pomelli, C.; Ochterski, J. W.; Ayala, P. Y.; Morokuma, K.; Voth, G. A.; Salvador, P.; Dannenberg, J. J.; Zakrzewski, V. G.; Dapprich, S.; Daniels, A. D.; Strain, M. C.; Farkas, O.; Malick, D. K.; Rabuck, A. D.; Raghavachari, K.; Foresman, J. B.; Ortiz, J. V.; Cui, Q.; Baboul, A. G.; Clifford, S.; Cioslowski, J.; Stefanov, B. B.; Liu, G.; Liashenko, A.; Piskorz, P.; Komaromi, I.; Martin, R. L.; Fox, D. J.; Keith, T.; Al-Laham, M. A.; Peng, C. Y.; Nanayakkara, A.; Challacombe, M.; Gill, P. M. W.; Johnson, B.; Chen, W.; Wong, M. W.; Gonzalez, C.; and Pople, J. A. *Gaussian 03*, Revision E.01; Gaussian, Inc.: Wallingford, CT, 2004.

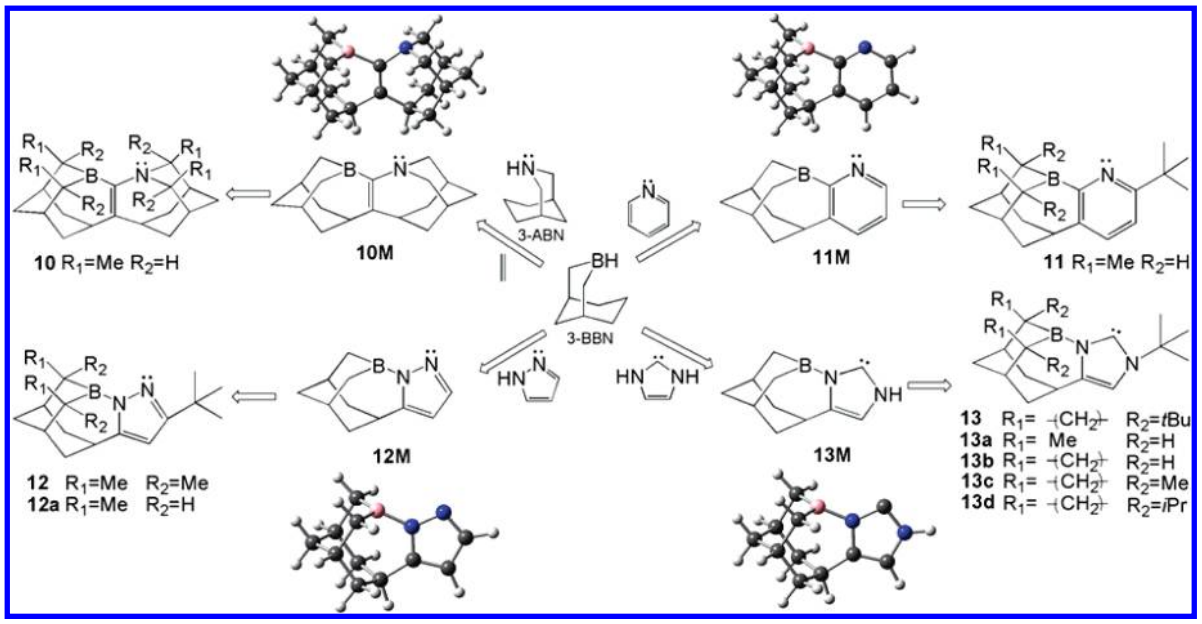

Figure 1. Constructions of molecules with desired hydrogen activation sites.

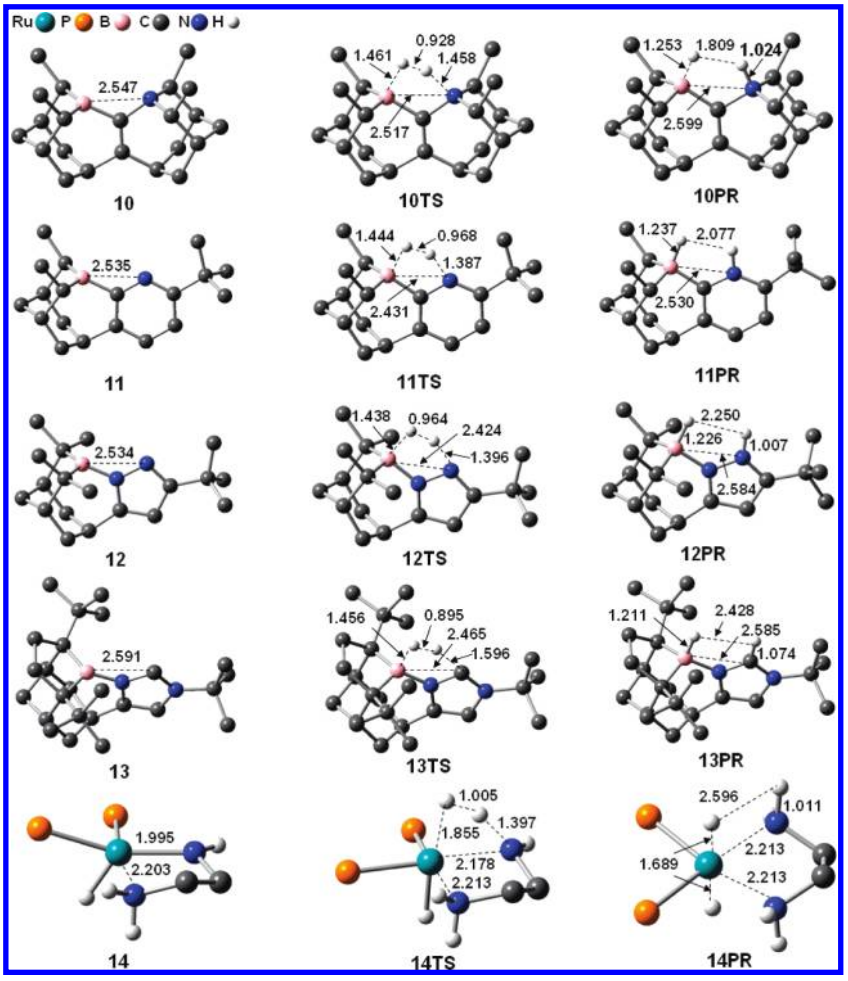

Figure 2. Optimized structures of **10**−**14**, the transition states (**10TS**−**14TS**) and the products (**10PR**−**14PR**). Some trivial hydrogen atoms are omitted for clarity.

the products (**10PR**−**13PR**) are shown in Figure 2. In agreement with our hypothesis, the dihydrogen fragments in **10TS**−**13TS** are coplanar to the B···N or B···C axes. Their energetic results are compared with those of the previously reported systems in Table 1. The geometric results of these previous systems are provided in Supporting

Table 1. Relative Enthalpies and Free Energies (kcal/mol) of H_2 Activation by the Designed Molecules (**10**−**13**) in Toluene, in Comparison with Those of Previously Reported Systems[a]

	transition state		product		
molecule	$\Delta H^{\ddagger}$	$\Delta G^{\ddagger}$	ΔH	ΔG	reference
10	3.8[b]	13.5	−11.8	−2.7	this work
11	5.8	15.4	−16.7	−7.8	this work
12	5.9	15.4	−22.6	−12.7	this work
13	5.4	15.5	−43.0	−32.9	this work
14	7.8	17.2	−14.4	−5.1	11
1[c]	3.7	13.1	−28.2	−19.8	5a 10a
3	27.3	36.0	−53.4	−44.6	12
4	21.2	31.6	−32.9	−22.9	13
7	14.5	22.9	−18.4	−10.1	14
8	6.8	16.4	−9.9	−0.8	14
9	11.0	23.2	−7.0	3.8	14

[a] The values in the gas phase are given in Supporting Information, SI3. [b] All values are relative to the separated reactants except for those of **1** which is relative to the P···B complex + H_2. [c] The ultrafine integration grid was used to reduce numerical uncertainty in the flat regions of the PES.

Information, SI3. The activation free energies ($\Delta G^{\ddagger}$) of **10**−**13**, 13.5, 15.4, 15.4, and 15.5 kcal/mol, respectively, are significantly lower than those of the experimental systems, 36.0 and 31.6 kcal/mol for **3** and **4**, respectively. The barriers are also lower than the 23.2 kcal/mol of the sp^3 carbon bridged FLP (**9**). However, they are marginally (or slightly) less reactive than **1** ($\Delta G^{\ddagger}$ = 13.1 kcal/mol). Experimentally, the acidic borane ($B(C_6F_5)_3$ are often used as acidic components of FLPs because the great acidity of borane can enhance the hydrogen activation. In our designed molecules, the B-center is less acidic than that in borane, but they have activation barriers comparable with the borane-paired FLPs (e.g., **4**). This further indicates the enhanced acid/base bifunctional reactivity in the designed active sites.

Figure 3 compares the orientations of the two critical molecular orbitals (MOs) (i.e., the boron vacant orbital (lowest unoccupied MO (LUMO)), and the N/P lone pair (highest occupied MO, HOMO)) in **1**, **9**, and **10**. Note that, to show the relative orientations of the MOs, we drew the two types of orbital in the same molecular frame. The difference between **I** and **III** shown in Scheme 2 can be observed (see **9** and **10** in Figure 3). According to the MOs of **1**, one may ask that the head-to-head orientations of the two orbitals do not look optimal for hydrogen activation, but it still has low barrier. This can be rationalized in terms of the so-called distortion energies[19] Because **1** is a weak nonbonding complex, it would require less energy to adjust itself to be prepared for H_2 activation. Using a similar measure proposed by Pápai and co-workers,[10c] the distortion energy of **1**, 6.2 kcal/mol, is less than the 8.0 (**10**), 10.5 (**11**), 11.5 (**12**) and 11.2 kcal/mol (**13**). Because the transition state of the sp^3 carbon bridged **9** is less ideal than those of **10**−**13**, it has larger distortion energy, 12.5 kcal/mol.

(19) Our distortion energy is defined as the energy difference between a free molecule and the corresponding frozen moiety in the transition state. For **1**, this is different from the approach proposed in ref 10c, the reported value (2.4 kcal/mol) is the difference between interaction energy of **1** and that of the frozen **1** moiety in the transition state. The authors used two set of reference monomers to calculate the two interaction energies. In our cases, **10**−**13** are not pairs (unlike **1**, the acidic and basic centers are incorporated in the same molecule), we thus calculated the distortion energies as defined. Our value of **1** (6.2 kcal/mol) can be obtained via the same approach of ref 10c but using the same reference monomers.

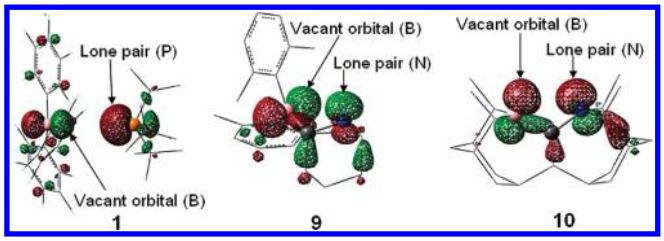

Figure 3. Comparisons of the relative orientations of the B vacant orbital and the N lone pair orbital in **1**, **9**, and **10**. Note that, to show the relative orientations of the two types of orbitals, they are drawn in the same molecular frame.

Similar to some FLPs,[8] one of the potential applications of these molecules is to perform direct metal-free hydrogenation. Currently, direct hydrogenations are predominately catalyzed by MLBHCs. The hydrogen activation step is the rate-determining step for MLBHC-catalyzed hydrogenations. The Ru-containing MLBHCs (e.g., **2**) are the often used catalysts. Like the previous studies,[11f,20] we used **14** (see Figure 2) as a computational model to study the reactivity of the Ru-containing MLBHCs. At the similar computational level,[21] the barrier of **14** ($\Delta G^{\ddagger}$ = 17.2 kcal/mol, which is in the range of 16.6−22.0 kcal/mol reported previously[22]) is compared with those of **10**−**13** (13.5−15.5 kcal/mol). Note that the barrier of a real catalyst (e.g., **2**) should be higher than the estimated value according to the model **14**, because accommodating a dihydrogen into a real catalyst would cause larger strain than in a model. Indeed, the activation free energy of the model **8**, 16.4 kcal/mol, is less than the 23.2 kcal/mol of **9** and that of the model **7**, 22.9 kcal/mol less than the 31.6 kcal/mol of **4**. Therefore, it can be conservatively concluded that **10**−**13** are more kinetically favorable than **2** in activating hydrogen molecule. The hydrogen activations of **10**−**12** also have comparable thermodynamics with that of **14**. Their exothermicities (ΔG), −2.7 (**10**), −7.8 (**11**), −12.7 (**12**), are close to the −5.1 kcal/mol of **14**. Therefore, when reacting with H_2, the designed molecules and the Ru-containing MLBHCs could behave similarly. Table 1 also includes the enthalpy results. The above conclusions also hold true in terms of their enthalpies.

Recently, Pápai's group[10d] has systematically investigated the kinetics and thermodynamics of various FLP hydrogen activations. In agreement with the experimental observations, they found that the reversible hydrogen activations of FLPs are slightly exothermic, the predicted ΔG values of $(o\text{-}C_6H_4Me)_3P/B(p\text{-}C_6F_4H)_3$,[5b] 1,8-bis(diphenylphosphino)naphthalene/$B(C_6F_5)_3$,[8a] and $Mes_2P-C_6F_4-B(C_6F_5)_2$[4a] are −0.1, −2.1, and −2.5 kcal/mol at the M05−2X/6-311++G**//M05−2X/6-31G* level in toluene, respectively. Thus, **10** has thermodynamics (ΔG = −2.7 kcal/mol) comparable with these experimental systems. The ΔG values of **11** (−7.8) and **12** (−12.7 kcal/mol)

(20) (a) Hedberg, C.; Kallstrom, K.; Arvidsson, P. I.; Brandt, P.; Andersson, P. G. *J. Am. Chem. Soc.* **2005**, *127*, 15083. (b) Chen, Y.; Tang, Y. H.; Lei, M. *Dalton Trans.* **2009**, 2359.

(21) For the Ru-containing model **14**, the calculations were performed using the M05-2X functional in combination with the basis sets of 6-311++G** for H, C, N, P and aug-cc-pVTZ for Ru.

(22) Using the mPW1PW91 functional in combination with the SDD basis set for Ru and 6-311++G** for H, N, C, and P, De Iuliis et al. predicted the activation free energy of model **14** to be 16.6 kcal/mol (see ref 11f); Hedberg et al. reported an activation free energy of 17.8 kcal/mol at B3LYP/LACV3P+**//B3LYP/LACVP** level (see ref 20a); Chen et al. predicted the barrier to be 22.0 kcal/mol using B3LYP functional with 6-31+G** for H, N, C, P and LANL2DZ for Ru (see ref 20b).

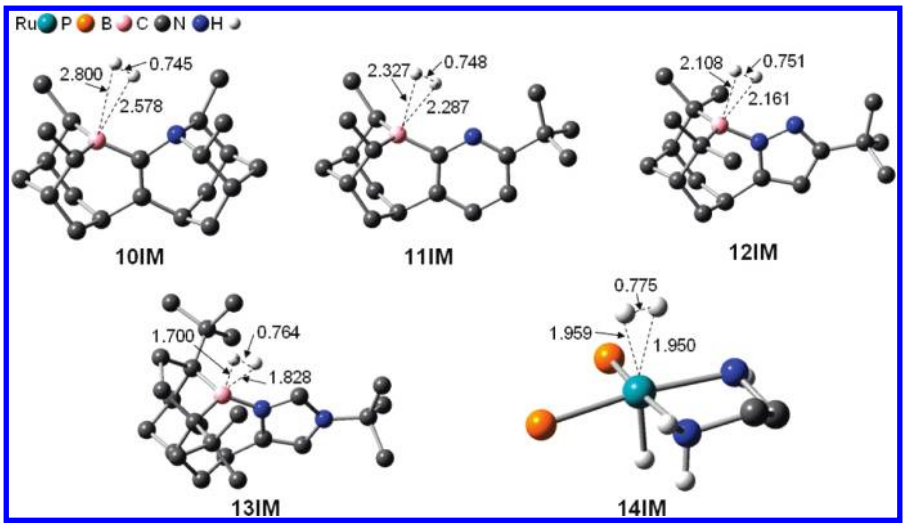

Figure 4. Optimized structures of the dihydrogen complexes.

seem to be somewhat too large for reversible hydrogen activations. However, we noticed that the experimentally reversible TMPN−CH_2−C_6H_4−$B(C_6F_6)_2$[8b] was computed to have a free energy of −12.5 kcal/mol at M05−2X/6-311++G**//M05−2X/6-31G* level in toluene[10d] and −7.3 kcal/mol at PBE/6-31G* level in benzene.[8b] Similar to the stable B/C: FLPs,[6] **13** is too exothermic to be reversible. Because the FLPs (e.g., 1,8-bis(diphenylphosphino)naphthalene/$B(C_6F_5)_3$) used for hydrogenation and the Ru-containing MLBHC model (**14**) have reversible or nearly reversible hydrogen activations, we reasoned that the favorable kinetics and the reversible (or nearly reversible) thermodynamics of **10**−**12** are implications that they can be further developed as metal-free hydrogenation catalysts. In the imine hydrogenations, the activated hydrogen atoms are often transferred to a C═N double bond via stepwise hydrogen transfer (proton transfer and then hydride transfer). In the ketone hydrogenations, the hydrogen atoms are often transferred to a C═O double bond concertedly. The two activated hydrogen atoms in **10PR**−**12PR** are also positioned like those in the hydrogen activation products of MLBHCs (see **14PR** in Figure 2). This is an advantage for the products to further react with unsaturated substrates. The FLP prototype **1** has more favorable kinetics than our designed molecules and **14**. However, the large exothermicity ($\Delta G = -19.8$ kcal/mol) could limit its application to perform catalytic hydrogenations because of a difficult hydrogen transfer step indicated by the large ΔG. Furthermore, the two activated hydrogen atoms in the product of **1** are head-to-head, forming a zwitterion. The ionic interaction can also prevent a facile hydrogen transfer step. To our knowledge, **1** has not been used to perform catalytic hydrogenation experimentally.

On the pathway of the hydrogen activation of **14**, a dihydrogen complex (**14IM**) prior to the transition state can be located computationally. Similar energy minima (**10IM**−**13IM** in Figure 4) can also be optimized for the reactions of **10**−**13** with H_2. However, the H−H bond lengths in **10IM**−**12IM** is only slightly elongated, 0.745 (**10IM**), 0.748 (**11IM**), and 0.751 Å (**12IM**), in comparison with 0.739 Å of free H_2. This suggests that these minima are not strict complexes. In contrast, because of the strong back-donation effect of Ru, the H−H bond in **14IM** is stretched substantially (0.775 Å). Nevertheless, because the binding free energies of these complexes, 5.2 (**10IM**), 5.1 (**11IM**), 5.3 (**12IM**), and 6.8 kcal/mol (**14IM**), are all positive, the computed complexes cannot be experimentally detected and should have no essential influences on the kinetics and thermodynamics of their hydrogen activations. Because of the stronger electron donation effect of carbene carbon than nitrogen, the H−H bond length (0.764 Å) in **13IM** is longer than the values in **10IM**−**12IM**, but it has more positive binding free energy (12.4 kcal/mol). Thus, in terms of reaction pathway, our molecules are also similar to the MLBCs. The positive binding free energies for **10IM**−**14IM** are majorly due to the thermal and entropic corrections. Without any corrections, the electronic binding energies of **10IM**−**12IM** and **14IM** are −2.1, −3.1, −3.9, and −3.0 kcal/mol, respectively. Thus the small negative values are not large enough to compensate the large positive corrections. Note that the hydrogen activation process is highly entropically unfavorable. However, in the case of **13IM**, the electronic binding energy is still positive (2.0 kcal/mol), which indicates the strains due to bonding the dihydrogen species are also contributors.

Summary

In conclusion, we have proposed a new pattern of hydrogen activation site based on our previously proposed sp^3 carbon bridged FLP. The new pattern was demonstrated achievable. The hydrogen activations of the designed molecules have better kinetics and thermodynamics than that of the sp^3 carbon bridged FLPs. Among the reported molecules, the hydrogen activations of **10**−**12** are kinetically and thermodynamically comparable with that of the Ru-containing MLBHC(**14**). Furthermore, the two activated hydrogen atoms in the products **10PR**−**12PR** are positioned properly for a subsequent hydrogen transfer step in the catalytic hydrogenations. These energetic and geometric features indicate that the new pattern of hydrogen activation site can be based to develop metal-free hydrogenation catalysts. The reported molecules could be the targets for experimental realizations.

Acknowledgment. This study was supported by the Chinese Academy of Sciences and NSFC (No: 20773160

and 20973197). We thank Prof. Pápai for explaining their energy partition scheme.

Supporting Information Available: Structures and orbital orientations of **10M**−**13M** (SI1); verifications of the possible dimers (SI2); the geometric and energetic results for reactions of **1**−**5** and 9 with H_2 (SI3); Cartesian coordinates of **10**−**14**, **10TS**−**14TS**, and **10PR**−**14PR** (SI4). This material is available free of charge via the Internet at http://pubs.acs.org.